INTEGRATED OPTICAL MODEL FOR STRAY LIGHT SUPPRESSION AND END-TO-END PERFORMANCE SIMULATION FOR GOCI

Sun-Jeong Ham[1,2], Jae Min Lee[1], Heong-Sik Youn[2], Gm Sil Kang[2,3], Seonghui Kim[2,3] and Sug-Whan Kim[1]

[1]SOL. Dept. of Astronomy and Space Science, Yonsei University
Sin Chon-dong Seodaemun-gu, Seoul , KOREA
Email: redion81@gmail.com

[2]Korea Aerospace Research Institute
45 Eoeun-dong Yuseong-gu Daejon Korea
Email: youn@kari.re.kr
sjham@kari.re.kr

[3]Astrium
31 Avenue des cosmonautes
31402 Toulouse Cedex 4

ABSTRACT KARI is currently developing a geostationary ocean color imager (GOCI) for COMS. We report the progress in integrated optical modeling and analysis for stray light suppression and the end-to-end instrument performance verification including in-orbit calibration. The Sun is modeled as the emitting light source and the selected area around Korean peninsular as the observation target that scatters the sun light towards GOCI in orbit. The optical ray tracing employing active geometric scaling was then used for precise characterization of the spatial and radiometric performance at the instrument focal plane. The analysis results show positive reduction in the simulated stray light level with the design improvement including baffles. It also indicates that the ray traced in-orbit radiometric performances are effective tools for the independent assessment of more traditional linear and quadratic equation based estimation of water leaving radiance. The concept of integrated GOCI optical model and the computational method are presented.

KEY WORDS: GOCI, COMS, stray light, calibration, end-to-end performance simulation

1. INTRODUCTION

"The COMS contract to develop the COMS satellite and to provide support for system activities has been awarded by KARI to ASTRIUM France. The COMS joint project group is composed of KARI and ASTRIUM engineers."

GOCI(Geostationary Ocean Color Imager), one of two science payloads of COMS, is a visible channel instrument. Its primary mission objective is to monitor the coastal water environment around the Korean peninsula. The GOCI development is currently progressing well and the critical design review is scheduled to February 2007. This will be followed by the manufacture, integration and test throughout 2007, which will bring the instrument to the ground calibration in late 2007 and early 2008.

As an important part of the GOCI development, we are building an end-to-end simulation tool for the GOCI in-orbit performance verification[1]. The computational technique embedded in the simulation tool employs an advanced ray tracing method that is radically different from the existing studies for end-to-end performance investigations [2, 3, 4].

This study addresses broadly two technical issues; the first is stray light suppression and the second the simulation of in-orbit measurement of water leaving radiance. Chapter 2 deals with the optical model construction and optical performance verification of GOCI instrument. This is followed by the initial study of in-field and near field stray lights when observing the extended area such as the target Korean peninsular. The first order stray light paths, their radiometric characteristics and the proposed ways of suppressing them are discussed in Chapter 3. The simulation technique for in-orbit measurement of water leaving radiance is demonstrated in Chapter 4, before it is concluded with the implications of the work to the on-going GOCI development in Chapter 5.

2. GOCI OPTICAL MODEL

2.1 GOCI optical system

The GOCI optical design with the one element filter assembly was initially proposed by Bevillon and Archer [5]. This initial design was later revised, using the first order estimation of image formation, to the new optical design with two element filter assembly for a better performance in reduction of ghost image at the focal plane [6]. For the purpose of stray light study and in-orbit measurement simulation, the later design was once again translated to a full 3D optical model as shown in Fig. 1.

This new model is intended to takes the full advantage of powerful ray tracing algorithm incorporated into the ASAP modelling environment [7, 8].
The pointing mirror reflects the incident light to the primary mirror (M1). It is then reflected, in turn, by the secondary mirror (M2), the tertiary mirror (M3) and the folding mirror before it reaches to the filter assembly. Once passed the filter, it goes through the detector window and, finally, ends at the detector surface. The optical system has the instant field of view of 1.03 degree, providing the single snap shot image of around 640 km x 640 km square area of the earth surface from the geostationary orbit. The single observation run is completed with a mosaic of 16 snap shot observation tiles (i.e. 4 x 4 tile array), using the motorised mechanism incorporated in the pointing mirror.

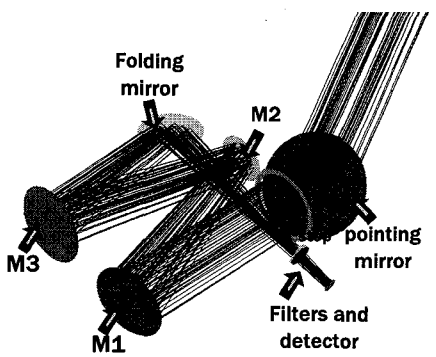

Figure 1. GOCI optical model translated from the original design by Bevillon & Archer.

2.2 Optical performance verification

In the earlier study [9], it was reported that the translated optical model was fine-tuned so that its spot diagram, one of the imaging performance indicators, is almost identical to that of the original design by Bevillon & Archer [5]. In addition, we investigated, this time, the MTF performance in the East-West and North-South directions for both original and translated GOCI optical designs and the results are shown in Fig. 2.
The MTF values of the translated optical design matches very well to that of the original design over the spatial frequency range under consideration. The MTF values together with the spot diagrams reported earlier prove that the translated GOCI optical design used in the following analysis meets the design optical requirement successfully.

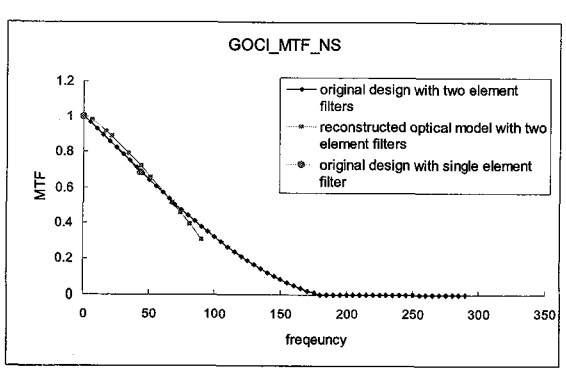

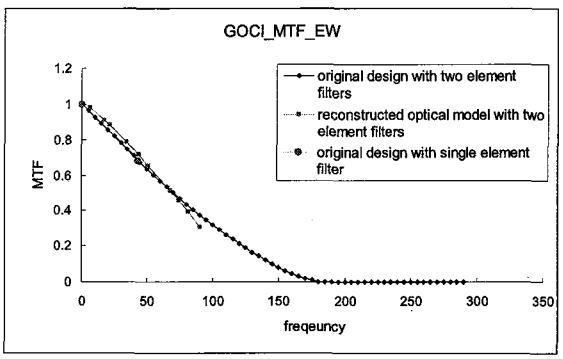

Figure 2. MTF plots against spatial frequency. The top graph shows N-S MTF, while the bottom is for E-W MTF.

3. STRAY LIGHT SUPPRESSION

3.1 In-field and near field stray light influences

One of the key stray light sources for GOCI is ironically the extended earth sphere flooding the entire GOCI aperture with the illumination. In this case, the observation target area, defined by the instant field of view, forms only a portion of the emitting surface area that illuminates the GOCI aperture at the geostationary orbit.
In order to find the optimum size for the emitting target surface area, we simulated the flux at the detector against the increasing target sampling area from 400 km x 400 km to about 1000 km x 1000 km as shown in Fig. 3. The resulting plots in Fig.4 indicate that the flux level at the detector plane increase with the target sampling area up until it reaches to 640 km x 640 km.
However, beyond that critical size, it is saturated at a constant level regardless the size of the observation tile. This gives us about 840 km x 840 km as the optimum size for the target area to be modelled as the combined in-field and near field scattering surface that send the scattered but converging beam to the GOCI aperture for the stray light analysis.

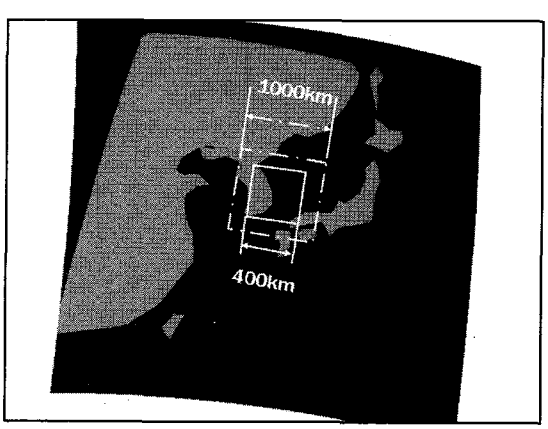

Figure 3. Increase in target area for flux simulation at the detector.

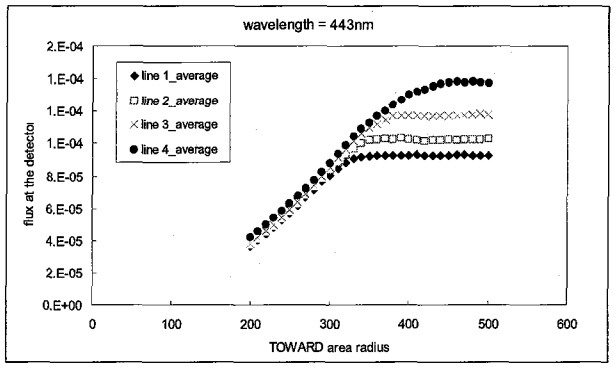

Figure. 4. Relative flux level vs increasing target sampling area. Each symbol denotes the averaged flux over the 4 observation tiles in the same latitude.

3.2 First order stray light reduction with baffle

Table 1 below lists key examples of the illuminated objects that are illuminated by the paraxial incident rays from the ideal grid source. The rays were traced in the forward direction from the aperture to the detector and those particular rays that deviate from the designed optical train were identified. With the addition of a baffle as shown in Fig. 5, those rays that are particularly threatening including the stray light path 5, 6 and 7 are successfully blocked.

It is worth noting that the stray light path 3, when viewed from the source, is caused by the small gap produced by the tilted pointing mirror and the rays run from the source to the infinity without hitting any object in the optical train in the model. This gap is filled with the baffle structure and the path 3 becomes one of non-threatening paths.

Table. 1. Key examples of illuminated objects and stray light reduction with baffle

Stray light path #	Path description	% of incident flux	% of incident flux baffle
3	From source to anywhere	5.71	Removed
5	From source to pointing mirror	4.42	Removed
6	From source to baseplate bottom	0.56	Removed
7	From pointing mirror to M2	0.16	Removed

We then performed the backward ray tracing all the ways from the detector to the entrance aperture in order to identify the critical objects that can be seen by the detector directly. A number of critical object were identified and, among them, the most threatening ray path 14 and 12 are listed in Table 2. These paths exist between the pointing mirror and M3, and it implies that the unwanted light incident onto the scan mirror can be re-directed to the detector via M3 with no obscuration at all.

The deployment of the baffle structure aforementioned removed these stray light paths successfully.

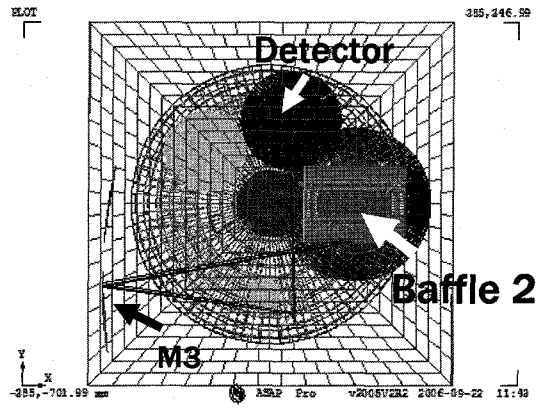

Figure 5. Addition of a proper baffle structure removes the most important stray light paths.

Table. 2. Key examples of critical objects and stray light reduction with baffle

Stray light path #	Path description	% of incident flux	% of incident flux with baffle
14	From M3 to pointing mirror	2.10	Removed
12	From M3 to pointing mirror	0.90	Removed

4. WATER LEAVING RADIANCE

4.1 Linear equation approach to flux correction

The measurement simulation of water leaving radiance from a selected area was performed with its part infected by the red tide. The total sampling area is around 840 km x 840 km in size, in which the red tide infection is spread to around 3.7×10^4 sq. km. For the definition of reflectance change caused by the red tide infection, the coupled ocean atmosphere radiative transfer model (COART) [10] was used to estimate the reflectivity (albedo) decrease from 0.055 (normal sea water) to 0.041 at the nominal wavelength 433nm with the Chlorophyll concentration of up to 10mg/cubic meter.

The end-to-end ray tracing was used to estimate the total flux level at the GOCI detector plane while the observation angle varied from 0 degree to 10 degree. The reference flux levels at the GOCI entrance aperture for the same observation configurations were obtained from either the following equation or the COART model [8]

$$F_{sc} = F_i \cdot \rho(\theta_i, \phi_i; \theta_s, \phi_s) \frac{A \cos\theta_e \cos\theta_s}{R^2} \quad \text{Eq. (1)}$$

where F_i is the incident flux on a slot, ρ BRDF of a slot, A the sampling area, θ and ϕ are polar and azimuth angles, and the subscription e and s are scatter angle and the angle between scattered ray and sampling edge normal.[11]

The linear equation for flux correction is given as

$$Fx = a\,x\,F_d + b \qquad \text{Eq. (2)}$$

where Fx is the reference flux at the entrance aperture, Fd the flux level at the detector. Applying Eq 2 twice for the two observation angle previously mentioned gives a pair of two linear equations that yield the correction coefficients a and b.

4.2 Quadratic equation approach to flux correction

Alternatively, a second order quadratic equation can be used for the flux correction between the detector plane and the entrance aperture, as expressed in Eq. 3

$$Fx = c\,x\,F_d^2 + d\,x\,F_d + e \qquad \text{Eg (3)}$$

In this case, solving Equation 3 requires for the flux measurement to be performed at three different observation angles such as 0, 10 and 20 degrees for example. Employing Eq 1 and 3 three times gives a set of simultaneous quadratic equations that can be solvable for the coefficient c, d and e.

4.3 Water leaving radiance from red tide infection

For the estimation of the reference flux level at the GOCI entrance aperture, the irradiance estimation from the COART model [10] was used for the flux correction between the detector plane and the aperture. The water leaving radiance L from the target area can then be estimated using the following equation

$$L = Fx / (A\,x\,\Omega x\,T) \qquad \text{Eq (4)}$$

Where L is the water leaving radiance, Fx the total flux received at the GOCI entrance aperture, A the source area within the system field of view, Ω the solid angle subtended by the GOCI aperture as viewed from the source and T the transmittance of the optical path from the source to the GOCI system.
The application of Eq. 2, 3 and 4 together with the flux level at the GOCI detector plane obtained from the end-to-end ray tracing simulation yielded the final water leaving radiance from the coastal sea surface infected with the aforementioned red tide as shown in Fig. 6. It is shown that, for the observation angle of 0 degree, the clear sea water gives 45.42watt/m^2.sr while it changes to 43.443 watt/m^2.sr for the red tide infected sea water.

Table 3. Radiance estimation for clear water. Note that the quadratic model gives better approximation to the reference COART model.

Observing angle (degree)	COART model (W/m^2/sr/μm)	Linear model (W/m^2/sr/μm)	Quadratic model (W/m^2/sr/μm)
0	45.42	47.55423	43.27253
10	46.91	49.91240	45.63070
20	51.02	56.04642	51.76472

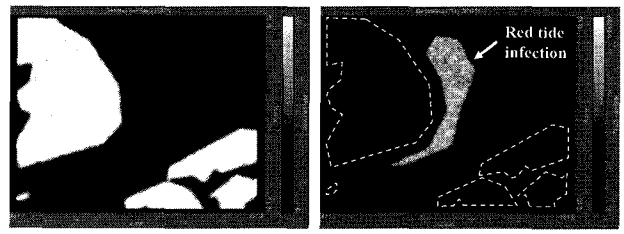

a. Before red tide | b. After red tide

Fig. 6 Images of normal clear sea water (left) and red tide infected water (right) with the water leaving radiance estimated using the end-to-end ray tracing simulation.

5. CONCLUDING REMARKS

Using the integrated end-to-end ray tracing model including the Sun (source), the Earth (target) and the instrument (GOCI), we investigated the stray light suppression and water leaving radiance measurement simulation for the in-orbit GOCI performance. The study demonstrates that the majority of primary stray light paths can be removed by the application of simple mechanical baffles. In addition, the integrated ray tracing model was successfully employed for the calibration of water leaving radiance.

References

[1] GOCI engineering team, "GOCI design review report", Astrium document, 2005.

[2] B. G. Crowther and S. R. Wassom, "Toward end-to-end optical system modeling and optimization; a step forward in optical design", Proc. of SPIE, Vol 5524

[3] M. W. Fitzmaurice, Kong Q. Ha, J. M. Howard, "End-to-end performance modeling of the James Webb Space Telescope (JWST) Observatory", Proc. of SPIE, Vol 5867

[4] S. W. Miller and W. R. Bergen, "End-to-end simulation for support of remote sensing system design", Proc. of SPIE, Vol 5548

[5] C. Bevillon, J. Archer et al., CodeV files, "TMA_GOCI_ss_GLB_ 150306.seq"

[6] Astrium document, COMS.TN.00149.DP.T.ASTR

[7] ASAP Primer 2005, Breault Research Organization

[8] ASAP online help, Breault Research Organization.

[9] S. J. Ham et al., "Integrated ray tracing model for in-orbit optical performance simulation for GOCI", Proc. of JC-SAT, 2006

[10] Coupled Ocean and Atmosphere Radiative Transfer (COART), http://snowdog.larc.nasa.gov/jin/rtset.html

[11] Jin, Z., T. Charlock, W. Smith Jr., and K Rutledge, " A parameterization of ocean surface albedo" , Geophysical Research Letters, November 2004, L22301